NUMERICAL MODELING OF A TURBULENT FLOW OVER A 2D CHANNEL WITH A RIB-ROUGHNEDE WALL

Rafael Gabler Gontijo, rafaelgabler@yahoo.com.br
José Luiz Alves da Fontoura Rodrigues, fontoura@unb.br
Universidade de Brasília, Departamento de Engenharia Mecânica, 70910-900, Brasília - DF

Abstract. *The heat transfer rates and velocity profiles in a turbulent incompressible flow of air over a 2D roughened sectioned rib channel were investigated by numerical simulation. The Reynolds number based on twice of the height channel is 37200 for the dynamic field and 12600 for the thermal field. The numerical results for the Nusselt number and velocity profiles are compared with experimental data. This test case is a generic flow used in the cooling systems of gas turbines. The ribs induce the flow separation, increasing the turbulence levels and, by consequence, the heat transfer. The numerical algorithm applies a consolidate Reynolds and Favre averaging process for the turbulent variables, and uses the classical $\kappa - \varepsilon$ model. The turbulent inner layer is modeled by four velocity and one temperature wall law. Spacial discretization is done by P1/isoP2 finite element method and temporal discretization is implemented using a semi-implicit sequential scheme of finite difference. The pressure-velocity coupling is numerically solved by a variation of Uzawa's algorithm. To filter the numerical noises, originated by the symmetric treatment to the convective fluxes, it is adopted a balance dissipation method. The remaining non-linearities, due to the laws of the wall, are treated by a minimal residual method.*

Keywords: *turbulence, heat transfer, rib channel, wall laws, finite element*

1. INTRODUCTION

The transport of thermal energy by turbulent flows happens in many situations of industrial interest. Despite the fact that turbulence is an unwished phenomenon for many applications in aerodynamics, it can be very useful in the project of heat exchangers. Artificial roughness elements, called "ribs", are used in many cooling system of gas turbines. Those ribs induce the flow separation, increasing the turbulence levels and, by consequence, the heat transfer rates. In this systems the cooling air enters from the root of the blade, flows along serpentine ducts and then exits at the back of the blade.

Patankar et. al (1977), Drain and Martin (1985), J.C. Han (1988), Liou et. al (1992),Iacovides et.al (1997) and M. Raisee (1997) have studied the ribbed channel and the differences between these works are basically in the geometry of the ribbed channel and in the Reynolds number of the flow. The ribbed channels studied in this work, are the ribbed channels of Drain and Martin (1985) and of Liou et. al (1992), both have the same geometry, but the first one studied only the dynamical field and with a Reynolds number based on twice of the channel height of 37200, while the second studied the thermal and dynamical field, with a Reynolds number of 12600. In the experimental work of Liou et. al (1992), the rib was made of aluminium and it was heated by a thermal film in its underside, providing a condition of constant heat flux. The top part of the channel was insulated, so an adiabatic wall was created. The height of the rib represents twenty percent of the height of the channel.

The main interest in the numerical modeling of this flow, is the prediction of the percentual raise in the heat transfer levels obtained by the introduction of the ribs. The efficiency of the mechanism depends on its geometry, on the thermodynamical properties of the fluid, and in the velocity field. The computational effort in order to simulate this kind of flow depends on the Reynolds number, in the relation between the height of the rib and the height of the channel and on the intensity of the temperature gradients involved.

In this work the numerical value of the local Nusselt number along the channel is calculated by the use of analogies between the friction and the heat transfer in the wall region. The value of the friction velocity is calculated in this work with the support of four different wall laws.

The solver used, named Turbo2D, is a research Fortran numerical code, that has been continuously devellopedby members of the Group of Complex Fluid Dynamics - Vortex, of the Mechanical Engineering Department of the University of Brasília, in the last twenty years. This solver is based on the adoption of the finite elements technique, under the formulation of pondered residuals proposed by Galerkin, adopting in the spatial discretization of the calculus dominium the triangular elements of the type P1-isoP2, as proposed by Brison, Buffat, Jeandel and Serres (1985). The isoP2 mesh is obtained by dividing each element of the P1 mesh into four new elements. In the P1 mesh only the pressure field is calculated, while all the other variables are calculated in the isoP2 mesh.

Considering the uncertainties normally existing about the initial conditions of the problems that are numerically simulated, it is adopted the temporal integration of the governing equations system. In the temporal integration process the initial state corresponds the beginning of the flow, and the final state occurs when the temporal variations of the velocity, pressure, temperature and other turbulent variables stop, in order to reach the final state, a pseudo transient occurs. The temporal discretization of the system of the governing equations, implemented by the algorithm of Brun (1988), uses se-

quential semi-implicit finite differences, with truncation error of order $0(\Delta t)$ and allows a linear handling of the equation system, at each time step.

The resolution of the coupled equations of continuity and momentum is done by a variant of Uzawat's algorithm proposed by Buffat (1981). The statistical formulation, responsible for the obtaining of the system of average equations, is done with the simultaneous usage of the Reynolds (1895) and Favre (1965) decomposition. The Reynolds stress tensor is calculated by the $\kappa - \varepsilon$ model, proposed by Jones and Launder (1972) with the modifications introduced by Launder and Spalding (1974). The turbulent heat flux is modeled algebraically using the turbulent Prandl number with a constant value of 0,9.

In the program Turbo2D, the boundary conditions of velocity and temperature can be calculated by four velocity and two temperature wall laws. The velocity wall laws used in this work are: the classical logarithm law, and the laws of Mellor (1966), Nakayama and Koyama (1984), and Cruz and Silva Freire (1998). The temperature wall law used is the Cheng and Ng (1982) wall law. The numerical instability resulted of the explicit calculus of the boundary conditions of velocity, trough the evolutive temporal process, is controlled by the algorithm proposed by Fontoura Rodrigues (1990). The numerical oscillations induced by the Galerkin formulation, resulting of the centered discretization applied to a parabolic phenomenon, that is the modeled flow, are cushioned by the technique of balanced dissipation, proposed by Huges and Brooks (1979) and Kelly, Nakazawa and Zienkiewicz (1976) with the numerical algorithm proposed by Brun (1988).

In order to quantify the wideness of range and the consistence of the numerical modeling done by the solver Turbo2D, the wall heat fluxes obtained numerically are compared to the experimental data of Drain and Martin (1985), and the velocity profiles are compared to the experimental data of Liou et. al (1992).

2. GOVERNING EQUATIONS

The system of non-dimensional governing equations, for a dilatable and one phase flow, without internal energy generation, and in a subsonic regime (Mach number under 0,3) is:

$$\frac{\partial \rho}{\partial t} + \frac{\partial (\rho u_i)}{\partial x_i} = 0, \tag{1}$$

$$\frac{\partial \rho u_i}{\partial t} + \frac{\partial}{\partial x_j}(\rho u_i u_j) = -\frac{\partial \underline{p}}{\partial x_i} + \frac{1}{Re}\frac{\partial}{\partial x_j}\left[\mu\left(\frac{\partial u_i}{\partial x_j} + \frac{\partial u_j}{\partial x_i}\right)\right] - \frac{2}{3Re}\frac{\partial}{\partial x_j}\left(\mu\frac{\partial u_k}{\partial x_k}\delta_{ij}\right) + \frac{1}{Fr}\rho\frac{g_i}{\|g\|}, \tag{2}$$

$$\frac{\partial (\rho T)}{\partial t} + \frac{\partial (\rho u_i T)}{\partial x_i} = \frac{1}{RePr}\frac{\partial}{\partial x_i}\left(k\frac{\partial T}{\partial x_i}\right) \tag{3}$$

$$\rho(T+1) = 1. \tag{4}$$

In this system of equations ρ is the fluid density, t is the time, x_i are the space cartesian coordinates in tensor notation, μ is the dynamic viscosity coefficient, δ_{ij} is the Kronecker delta operator, g_i is the acceleration due to gravity, T is the absolute temperature, u_i is the flow velocity , k is the thermal conductivity, Re is the Reynolds number, Fr is the Froud number, Pr is the Prandtl number, and the non dimensional pressure is:

$$\underline{p} = \frac{p - p_m}{\rho_o U_o^2} \tag{5}$$

Where p_m is the average spatial value of the pressure field, p is the actual value of pressure, ρ_0 and u_0 are the reference values of the fluid density and the flow velocity . More details about the dimensionless process are given by Brun (1988). In order to simplify the notation adopted, the variables in their dimensionless form have the same representation as the dimensional variables. The Reynolds, Prandtl and Froude numbers are defined with the reference values adopted in this process.

2.1 THE TURBULENCE MODEL

In this work all the dependent variables of the fluid are treated as a time average value plus a fluctuation of this variable in a determinate point of space and time. In order to account variations of density, the model used applies the well known Reynolds (1985) decomposition to pressure and fluid density and the Favre (1965) decomposition to velocity and temperature. In the Favre (1965) decomposition a randomize generic variable φ is defined as:

$$\varphi(\vec{x},t) = \widetilde{\varphi}(\vec{x}) + \varphi''(\vec{x},t) \qquad \text{with} \qquad \widetilde{\varphi} = \frac{\overline{\rho\varphi}}{\bar{\rho}} \qquad \text{and} \quad \overline{\varphi''}(\vec{x},t) \neq 0. \tag{6}$$

Applying the Reynolds (1895) and Favre (1965) decompositions, to the governing equations, and taking the time average value of those equations, we obtain the mean Reynolds equations:

$$\frac{\partial \overline{\rho}}{\partial t} + \frac{\partial}{\partial x_i}\left(\overline{\rho}\widetilde{u}_i\right) = 0, \tag{7}$$

$$\frac{\partial}{\partial t}\left(\overline{\rho}\widetilde{u}_i\right) + \frac{\partial}{\partial x_j}\left(\overline{\rho}\widetilde{u}_j\widetilde{u}_i\right) = -\frac{\partial \overline{p}}{\partial x_i} + \frac{\partial}{\partial x_j}\left[\overline{\tau_{ij}} - \overline{\rho u_j'' u_i''}\right] + \overline{\rho} g_i, \tag{8}$$

where

$$\overline{\tau_{ij}} = \mu\left[\left(\frac{\partial \widetilde{u}_i}{\partial x_j} + \frac{\partial \widetilde{u}_j}{\partial x_i}\right) - \frac{2}{3}\frac{\partial \widetilde{u}_l}{\partial x_l}\delta_{ij}\right], \tag{9}$$

$$\frac{\partial(\overline{\rho}\widetilde{T})}{\partial t} + \frac{\partial(\widetilde{u}_i\widetilde{T})}{\partial x_i} = \frac{\partial}{\partial x_i}\left(\alpha\frac{\partial \widetilde{T}}{\partial x_i} - \overline{\rho u_i'' T''}\right) \tag{10}$$

$$\overline{p} = \overline{\rho} R \widetilde{T} \tag{11}$$

In these equations α is the molecular thermal diffusivity and two news unknown quantities appear in the momentum (8) and in the energy equation (10), defined by the correlations between the velocity fluctuations, the so-called Reynolds Stress, given by the tensor $-\overline{\rho u_i'' u_j''}$, and by the fluctuations of temperature and velocity, the so-called turbulent heat flux, defined by the vector $-\overline{\rho u_i'' T''}$.

The Reynolds stress of turbulent tensions is calculated by the $\kappa - \varepsilon$ model, proposed by Jones and Launder (1972) with the modifications introduced by Launder and Spalding (1974), where

$$-\overline{\rho u_i'' u_j''} = \mu_t\left(\frac{\partial \widetilde{u}_i}{\partial x_j} + \frac{\partial \widetilde{u}_j}{\partial x_i}\right) - \frac{2}{3}\left(\overline{\rho}\kappa + \mu_t\frac{\partial \widetilde{u}_l}{\partial x_l}\right)\delta_{ij}, \tag{12}$$

with

$$\kappa = \frac{1}{2}\overline{u_i'' u_i''}. \tag{13}$$

and

$$\mu_t = C_\mu \bar{\rho}\frac{\kappa^2}{\varepsilon} = \frac{1}{Re_t} \ . \tag{14}$$

The turbulent heat flux is modeled algebraically using the turbulent Prandl number Pr_t equal to a constant value of 0,9 by the relation

$$-\overline{\rho u_i'' T''} = \frac{\mu_t}{Pr_t}\frac{\partial \widetilde{T}}{\partial x_i}. \tag{15}$$

In the equation (14) C_μ is a constant of calibration of the model, that values $0,09$, κ represents the turbulent kinetic energy and ε is the rate of dissipation of the turbulent kinetic energy. Once that κ and ε are additional variables, we need to know there transport equations. The transport equations of κ and ε were deduced by Jones and Launder (1972), and the closed system of equations to the $\kappa - \varepsilon$ model is given by:

$$\frac{\partial \bar{\rho}}{\partial t} + \frac{\partial(\bar{\rho}\widetilde{u}_i)}{\partial x_i} = 0 \ , \tag{16}$$

$$\frac{\partial\left(\bar{\rho}\widetilde{u}_i\right)}{\partial t} + \widetilde{u}_j\frac{\partial\left(\bar{\rho}\widetilde{u}_i\right)}{\partial x_j} = -\frac{\partial \bar{p}^*}{\partial x_i} + \frac{\partial}{\partial x_j}\left[\left(\frac{1}{Re} + \frac{1}{Re_t}\right)\left(\frac{\partial \widetilde{u}_i}{\partial x_j} + \frac{\partial \widetilde{u}_j}{\partial x_i}\right)\right] + \frac{1}{Fr}\bar{\rho} g_i \ , \tag{17}$$

$$\frac{\partial\left(\bar{\rho}\widetilde{T}\right)}{\partial t} + \widetilde{u}_j\frac{\partial\left(\bar{\rho}\widetilde{T}\right)}{\partial x_j} = \frac{\partial}{\partial x_j}\left[\left(\frac{1}{Re\,Pr} + \frac{1}{Re_t\,Pr_t}\right)\frac{\partial \widetilde{T}}{\partial x_j}\right] \ , \tag{18}$$

$$\frac{\partial\left(\bar{\rho}\kappa\right)}{\partial t} + \widetilde{u}_i\frac{\partial\left(\bar{\rho}\kappa\right)}{\partial x_j} = \frac{\partial}{\partial x_i}\left[\left(\frac{1}{Re} + \frac{1}{Re_t\,\sigma_\kappa}\right)\frac{\partial \kappa}{\partial x_i}\right] + \Pi - \bar{\rho}\varepsilon + \frac{\bar{\rho}\beta g_i}{Re_t\,Pr_t}\frac{\partial \widetilde{T}}{\partial x_i} \ , \tag{19}$$

$$\begin{aligned}\frac{\partial\left(\bar{\rho}\varepsilon\right)}{\partial t} + \widetilde{u}_i\frac{\partial\left(\bar{\rho}\varepsilon\right)}{\partial x_j} &= \frac{\partial}{\partial x_i}\left[\left(\frac{1}{Re} + \frac{1}{Re_t\,\sigma_\varepsilon}\right)\frac{\partial \varepsilon}{\partial x_i}\right] \\ &\quad + \frac{\varepsilon}{\kappa}\left(C_{\varepsilon 1}\Pi - C_{\varepsilon 2}\bar{\rho}\varepsilon + C_{\varepsilon 3}\frac{\bar{\rho}\beta g_i}{Re_t\,Pr_t}\frac{\partial \widetilde{T}}{\partial x_i}\right) \ ,\end{aligned} \tag{20}$$

$$\bar{\rho}\left(1 + \widetilde{T}\right) = 1 \ , \tag{21}$$

where:

$$\frac{1}{Re_t} = C_\mu \bar{\rho} \frac{\kappa^2}{\varepsilon} \ , \tag{22}$$

$$\Pi = \left[\left(\frac{1}{Re_t} \right) \left(\frac{\partial \widetilde{u}_i}{\partial x_j} + \frac{\partial \widetilde{u}_j}{\partial x_i} \right) - \frac{2}{3} \left(\bar{\rho}\kappa + \frac{1}{Re_t} \frac{\partial \widetilde{u}_l}{\partial x_l} \right) \delta_{ij} \right] \frac{\partial \widetilde{u}_i}{\partial x_j} \ , \tag{23}$$

$$p^* = \bar{p} + \frac{2}{3} \left[\left(\frac{1}{Re} + \frac{1}{Re_t} \right) \frac{\partial \widetilde{u}_l}{\partial x_l} + \bar{\rho}\kappa \right] \ , \tag{24}$$

with the model constants given by:

$$C_\mu = 0,09 \ , \ C_{\varepsilon 1} = 1,44 \ , \ C_{\varepsilon 2} = 1,92 \ , \ C_{\varepsilon 3} = 0,288 \ , \ \sigma_\kappa = 1 \ , \ \sigma_\varepsilon = 1,3 \ , \ Pr_t = 0,9 \ .$$

2.2 NEAR WALL TREATMENT

The $\kappa - \varepsilon$ turbulence model is incapable of properly representing the laminar sub-layer and the transition regions of the turbulent boundary layer. To solve this inconvenience, the solution adopted in this work is the use of laws of the wall for temperature and for velocity, capable of properly representing the flow in the inner region of the turbulent boundary layer.

There are four velocity and one temperature law of the wall implemented on Turbo 2D. The laws used in this simulation are shown bellow, except for the classical log law, that futher explanations are unnecessary.

2.2.1 Velocity law of the wall of Mellor(1966)

Deduced from the equation of Prandtl for the boundary layer flow, considering the pressure gradient term for integration, this wall function is a primary approach to flows that suffer influence of adverse pressure gradients. Its equations are, respectively, for the laminar and turbulent region

$$u^* = y^* + \frac{1}{2} p^* y^{*2} \ , \tag{25}$$

$$u^* = \frac{2}{K} \left(\sqrt{1 + p^* y^*} - 1 \right) + \frac{1}{K} \left(\frac{4y^*}{2 + p^* y^* + 2\sqrt{1 + p^* y^*}} \right) + \xi_{p^*} \ , \tag{26}$$

where the asterisk super-index indicates dimensionless quantities of velocity u^*, pressure gradient p^* and distance to the wall y^*, as functions of scaling parameters to the near wall region, K is the Von Karman constant, and ξ_{p^*} is Mellor's integration constant, function of the near-wall dimensionless pressure gradient, determined in his work of (1966).

The intersection of both regions is considered to be the same as the log law expressions, with $y^* = 11,64$. The relations between the dimensionless near wall properties and the friction velocity u_f are:

$$y^* = \frac{y\, u_f}{\nu} \quad , \quad u^* = \frac{\widetilde{u}_x}{u_f} \quad \text{and} \quad p^* = \frac{1}{\bar{\rho}} \frac{\partial \bar{p}}{\partial x} \frac{\nu}{{u_f}^3} \ . \tag{27}$$

The friction velocity is calculated by the relation:

$$u_f = \left(\frac{1}{Re} + \frac{1}{Re_T} \right) \frac{\partial u_i}{\partial x_j} - \frac{1}{\rho} \frac{\partial P}{\partial x_i} \delta_{ij} \tag{28}$$

In equation (26) the term ξ_{p^*} is a value obtained from the integration process proposed by Mellor (1966) and is a function of the dimensionless pressure gradient. Its values are obtained through interpolation of those obtained experimentally by Mellor, shown in table (1).

Table 1. Mellor's integration constant (1966)

p^*	$-0,01$	$0,00$	$0,02$	$0,05$	$0,10$	$0,20$	$0,25$	$0,33$	$0,50$	$1,00$	$2,00$	$10,00$
ξ_{p^*}	$4,92$	$4,90$	$4,94$	$5,06$	$5,26$	$5,63$	$5,78$	$6,03$	$6,44$	$7,34$	$8,49$	$12,13$

2.2.2 Velocity law of the wall of Nakayama and Koyama (1984)

In their work, Nakayama and Koyama (1984) proposed a derivation of the mean turbulent kinetic energy equation, that resulted in an expression to evaluate the velocity near solid boundaries. Using experimental results and those obtained by Strattford (1959), the derived equation is

$$u^* = \frac{1}{K^*}\left[3(t-t_s) + ln\left(\frac{t_s+1}{t_s-1}\frac{t-1}{t+1}\right)\right] \ , \tag{29}$$

with

$$t = \sqrt{\frac{1+2\tau^*}{3}} \quad , \quad \tau^* = 1 + p^* y^* \quad , \quad K^* = \frac{0,419 + 0,539p^*}{1+p^*} \quad and \quad {y^*}_s = \frac{e^{K\,C}}{1+p^{*0,34}} \ , \tag{30}$$

where K^* is the expression for the Von Karman constant modified by the presence of adverse pressure gradients, τ^* is a dimensionless shear stress, $C = 5,445$ is the log-law constant and t, ${y^*}_s$ and t_s, a value of t at position ${y^*}_s$, are parameters of the function.

2.2.3 Velocity law of the wall of Cruz and Silva Freire (1998)

Analyzing the asymptotic behavior of the boundary layer flow under adverse pressure gradients, Cruz and Silva Freire (1998) derived an expression for the velocity. The solution of the asymptotic approach is

$$u = \frac{\tau_w}{|\tau_w|}\frac{2}{K}\sqrt{\frac{\tau_w}{\rho} + \frac{1}{\rho}\frac{dp_w}{dx}y} + \frac{\tau_w}{|\tau_w|}\frac{u_f}{K}ln\left(\frac{y}{L_c}\right) \quad with \quad L_c = \frac{\sqrt{\left(\frac{\tau_w}{\rho}\right)^2 + 2\frac{\nu}{\rho}\frac{dp_w}{dx}u_f} - \frac{\tau_w}{\rho}}{\frac{1}{\rho}\frac{dp_w}{dx}} \ , \tag{31}$$

where the sub-index $_w$ indicates the properties at the wall, K is the Von Karman constant, L_c is a length scale parameter and u_f is the friction velocity.

The proposed equation for the velocity (31) has a behavior similar to the log law far from the separation and reattachment points, but close to the adverse pressure gradient, it gradually tends to Stratford's equation (1959). The same process was used to derive the temperature law of the wall by Cruz and Silva Freire (1998).

2.2.4 Temperature law of the wall of Cheng and Ng (1982)

For the calculation of the temperature, Cheng and Ng (1982) derived an expression for the near wall temperature similar to the log law of the wall for velocity. For the laminar and turbulent regions, the equations are respectively

$$\frac{(T_0 - T)_y}{T_f} = y^*\ Pr \quad \text{and} \quad \frac{(T_0 - T)_y}{T_f} = \frac{1}{K_{Ng}}ln(y^*) + C_{Ng} \ , \tag{32}$$

where T_0 is the environmental temperature and T_f is the friction temperature, as defined by Brun (1988):

$$T_f u_f = \left[\left(\frac{1}{RePr} + \frac{1}{Re_T Pr_T}\right)\frac{\partial \widetilde{T}}{\partial x_j}\right]_\delta \tag{33}$$

The intersection of these regions are at $y^* = 15,96$, and the constants K_{Ng} and C_{Ng} are, respectively, 0,8 and 12,5.

2.3 ANALOGIES EMPLOYED

In this work the wall heat flux is calculated in the non dimentional form of the Nusselt number, that for a channel can be calculated by the following relation:

$$Nu_x = \frac{2q_x^{''}PrH}{\mu C_p(T_w - T_{bulk})} \tag{34}$$

In the equation above, Nu_x represents the local Nusselt number, $q_x^{''}$ is the local heat flux per unit of area, Pr is the Prandtl number of the fluid, H is the height of the channel, and T_w is the temperature of the wall. In 1933 Colburn derived an expression from the Reynolds analogy, that establishes a relation between the local Stanton number, the local friction coefficient and the Prandtl number of the fluid, valid for fluids with Prandtl numbers up to 0,5. The semi-empirical expression derived by Colburn is:

$$St_x = \frac{Cf_x}{2Pr^{\frac{2}{3}}} \tag{35}$$

In the equation above, Cf_x represents the local friction coefficient, defined as:

$$\frac{Cf_x}{2} = \frac{\tau_{wx}}{\rho u_\infty^2} = \frac{\rho u_{fx}^2}{\rho u_\infty^2} = \frac{u_{fx}^2}{u_\infty^2} \tag{36}$$

Where, ρ is the density of the fluid, u_∞ is the free stream velocity of the flow, τ_w is the local shear stress on the wall and u_{fx} is the local friction velocity.

The Stanton number, by definition can also be expressed as:

$$St_x = \frac{q_x''}{\rho C_p u_\infty (T_w - T_\infty)} \tag{37}$$

Defining the bulk temperature as:

$$T_{bulk} = \frac{T_w + T_\infty}{2} \tag{38}$$

And combining equations (34),(35),(36),(37) and (38), it is possible to estabilish a relation between the local Nusselt number and the friction velocity, as:

$$Nu_x = \frac{4Pr^{\frac{1}{3}} u_{fx}^2 H}{\nu u_\infty} \tag{39}$$

The equation above was used to calculate the local Nusselt number along the ribbed channel. This methodology was successful employed by Gontijo and Fontoura Rodrigues (2006a and 2006b) for turbulent flows over flat plates with unheated starting lenghts.

3. NUMERICAL METHODOLOGY

The calculation domain used in the simulation is represented by the picture bellow.

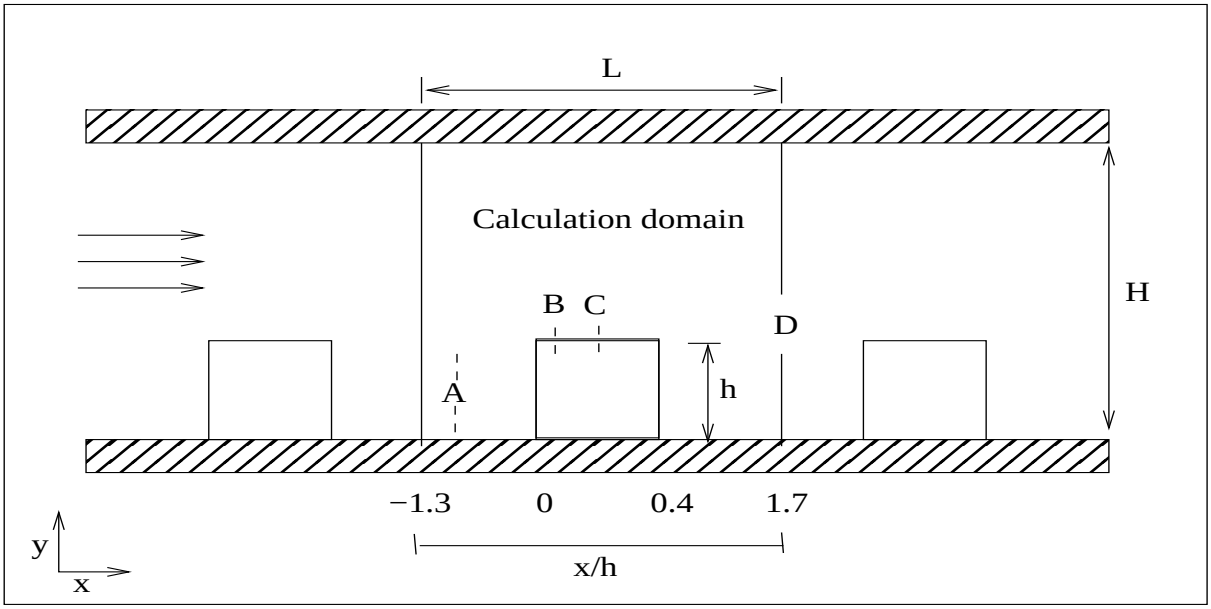

Figure 1. Calculation domain used in the simulation

In the picture above the values of the lenghts represented are: $H = 4cm$, $L = 5,76cm$ and $h = 0,8cm$. The points A,B,C and D, represent the sections where the profiles were taken, their coordinates are respectively -0.816x/h, 0.04x/h, 0.2x/h and 1.672x/h. The boundary inlet conditions are velocity, turbulent kinetic energy and ε experimental profiles, in the bottom wall a condition of constant heat flux was applied, in the top part an adiabatic wall was imposed, and a pressure difference was setted up between the inlet and the outlet. The boundary wall velocity in the bottom part is calculated with the wall laws, in a distance about $y^+ = 1.5$.

The meshes used in the simulation consists in a P1 mesh with 970 nodes and 1800 elements, and a isoP2 mesh with 3739 nodes and 7200 elements. Those meshes are shown in the picture bellow:

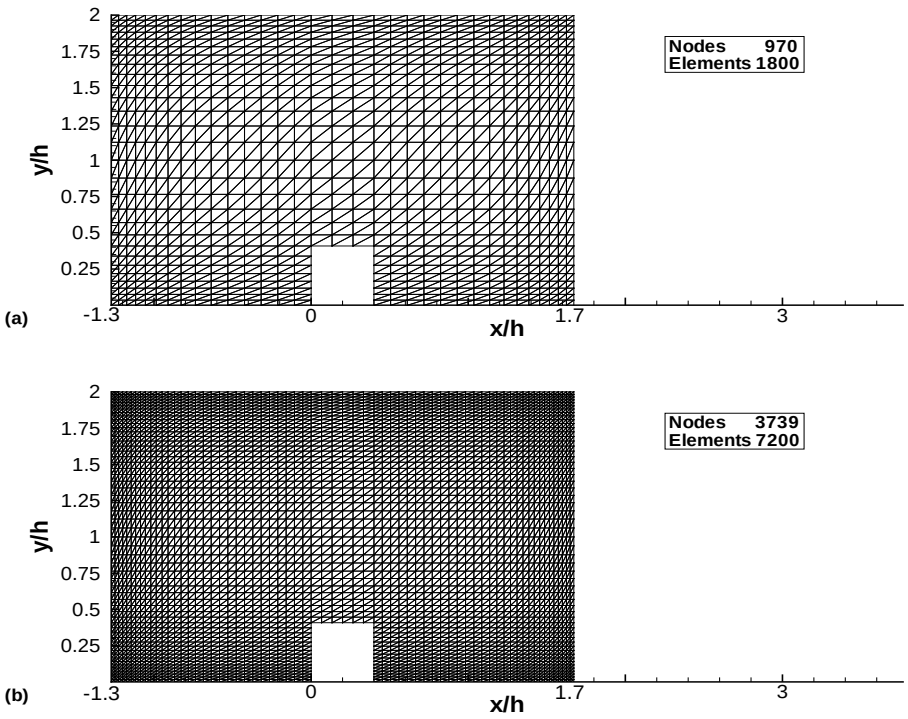

Figure 2. P1 mesh (a), and IsoP2 mesh (b)

4. NUMERICAL RESULTS

The first interesting qualitative result presented are the velocity fields and the recicurlation regions obtained with the use of four different velocity wall laws.

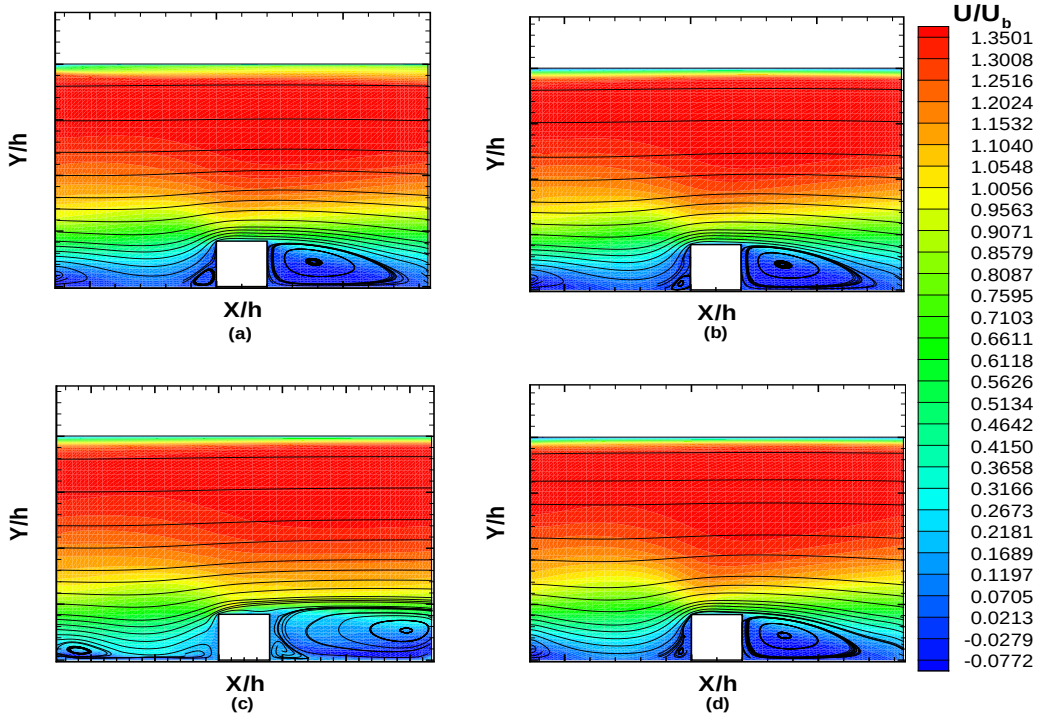

Figure 3. Velocity fields and the recirculating regions. (a) log law, (b) law of Mellor, (c) law of Koyama and Nakayama, (d) law of Cruz and Silva Freire

In the figure 3, U_b is the velocity in wich the Reynolds number of the flow was based, in this case it's value is $7,4m/s$. It is possible to notice from the picture above that there are considerable differences between the velocity profiles calculated with the law of Koyama and Nakayama and the other laws.

Figure 4 shows the velocity profiles obtained in four different locations of the channel, respectively points A,B,C and D (shown in figure 1). The numerical results are compared to the experimental data of Drain and Martin (1985).

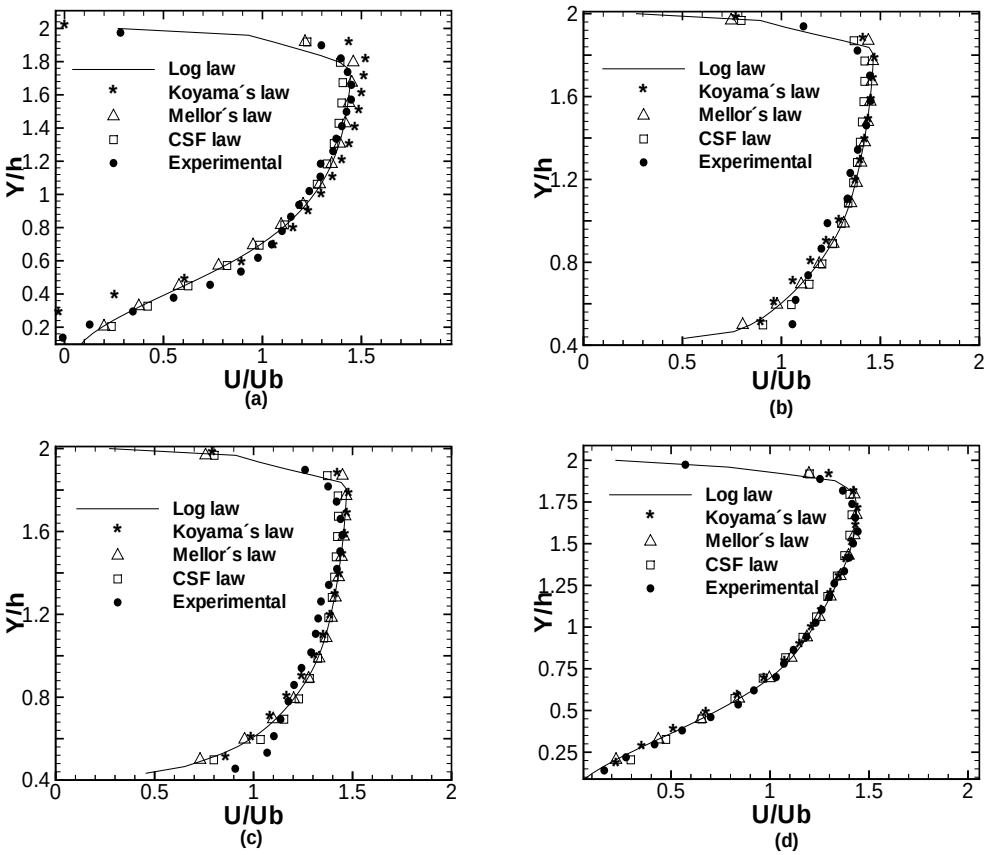

Figure 4. Velocity profiles in the positions: (a) x/h=-0.816 - A, (b) x/h=0.04 - B, (c) x/h=0.2 -C, (d) x/h=1.672 - D

In figure 4, the profiles presented in letters (b) and (c) are taken above the rib, it is possible to notice that the Koyama's law presents a good aproach with the experimental results in this region, while before and after the rib, in the recirculating regions, this law is the one that produces the worse results. The other three wall laws tested produces very similar results for the velocity field, and they all are capable to predict with a great precision the dynamical behavior of this complex flow.

The next picture shows the pressure and the tubulent kinetic energy fields.

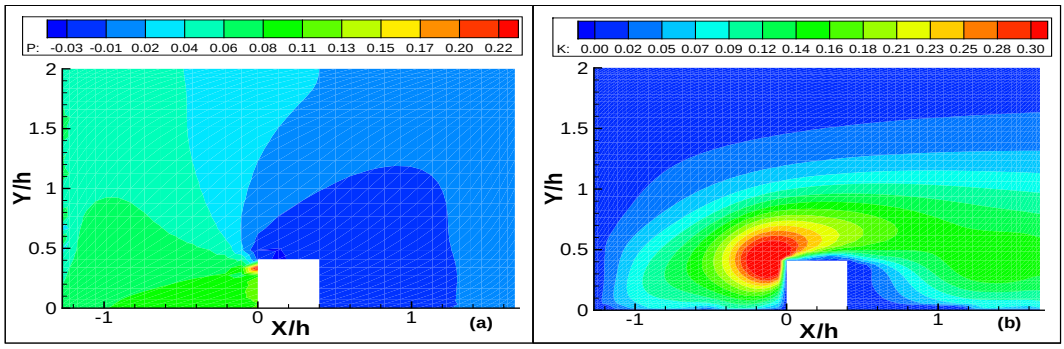

Figure 5. Pressure (a), and turbulent kinetic energy (b) fields

It is possible to notice in figure 5 that a low pressure zone occurs in the recirculation region after the rib, and that a high turbulent kinetic energy intensity is observed in the beggining of the rib. The high values of κ are related with high turbulence intensity and by consequence with a higher heat transfer rate, since turbulence converts kinetic energy into heat, this will be better visualized in figure 6.

The next analisys is done for the heat transfer along the bottow wall, where the rib is located.

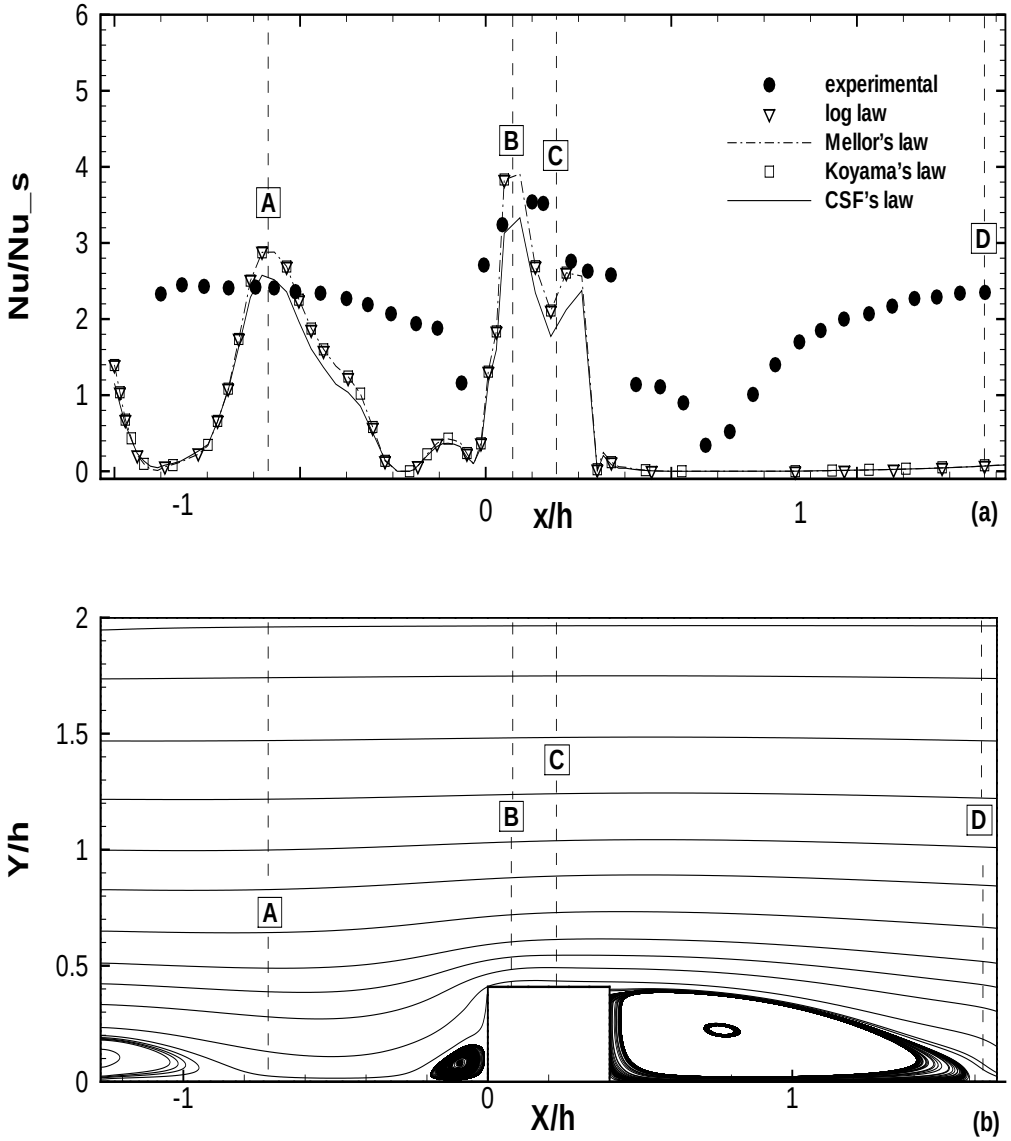

Figure 6. Nusselt number along the bottom wall (a), structure of the recirculation regions (b)

In order to quantify the raise in the heat transfer rates between the wall and the flow, induced by the presence of the rib, figure 6 shows how the relation between the local Nusselt number, Nu_x, and the Nusselt number for a non ribbed channel, Nu_s, changes along the calculation domain. The mean Nussel number for a non ribbed channel is calculated by the Dittus-Boelter correlation:

$$Nu_s = 0.023 Re^{0.8}.Pr^{0.4} \tag{40}$$

The numerical and experimental values of the Nusselt number along the channel are in good agreement in the non recirculating regions. The most important parameter of engineering interest to be obtained is the maximum relation between the local Nusselt number (Nu_x) and the Nusselt number obtained with the Dittus-Boelter correlation (Nu_s), because this relation gives the idea of how the heat transfer is increased by the use of the rib. In this simulation the values obtained for the highest value of the Nusselt number are very closed to the experimental data.It's important to notice that the introduction of the rib in the channel increases in 3.5 times the heat transfer between the channel and the cooling air.

5. CONCLUSIONS

From the comparation between the numerical and experimental results, it is possible to conclude that the numerical methodology employed in this work is capable to predict well the behavior of the velocity field.

For the heat transfer rates, in the non recirculating regions, points A,B and C (defined in figure 1), the agreement between the numerical and experimental values is good. In the regions of boundary layer deattachment, before and after the rib, the numerical values show heat transfer levels under the experimental results.

It is important to remind that the Colbun analogy produces great results in flows where the turbulence is in equilibrium between production and dissipation, what does not happens in the bottom part of the flow, where the two recirculation regions appear.

The implementation in the Turbo2D code of analogies that better represents the turbulent difusion of momentum and heat in the recirculating regions, could raise considerable the quality of the resulting numerical modeling.

6. REFERENCES

ABCM, 2004, "Journal of the Brazilian Society of Engineering and Mechanical Sciences", http://www.abcm.org.br/journal/index.shtml. Boussinesq, J., 1877, "Théorie de lt'Écoulement Tourbillant" , Mem. Présentés par Divers Savants Acad. Sci. Inst. Fr., vol. 23, pp. 46-50.

Bejan, A., 1994, "Convective Heat Transfer", John Wily and Sons, USA.

Buffat, M., 1981, "Formulation moindre carrés adaptées au traitement des effets convectifs dans les équation de Navier-Stokes", Doctorat thesis, Université Claude Bernard, Lyon, France.

Brison ,J. F., Buffat, M., Jeandel,D., Serrer,E., 1985, "Finite elements simulation of turbulent flows, using a two equation model", Numerical methods in laminar and turbulent flows, Swansea. Pineridg Press.

Brun, G., 1988, "Developpement et application dt'une methode dt'elements finis pour le calcul des ecoulements turbulents fortement chauffes " , Doctorat thesis, Laboratoire de Mécanique des Fluides, Escola Central de Lyon.

Cheng, R.K. and Ng, T.T., 1982, "Some aspects of strongly heated turbulent boundary layer flow". Physics of Fluids, vol. 25(8).

Colburn, A.P., 1933 , "A method for correlating forced convection heat transfer data and a comparison with fluid friction " Transaction of American Institute of Chemical Engineers, vol. 29, pp. 174-210.

Cruz, D.O.A., Silva Freire, A.P., 1998, "On single limits and the asymptotic behavior of separating turbulent boundary layers", International Journal of Heat and Mass Transfer, vol. 41, n^o 14, pp. 2097-2111

L.D. Drain and S. Martin. Two-component velocity measurements of turbulent flow in a ribbed-wall flow channel. In Int. Conf. on Laser Anenometry - Advances and Application, 1985.

Favre, A., 1965, "Equations de gaz turbulents compressibles". Journal de mecanique, vol. 3 e vol. 4.

Fontoura Rodrigues, J. L. A., 1990, "Méthode de minimisation adaptée à la techinique des éléments finis pour la simulation des écoulements turbulents avec conditions aux limites non linéaires de proche paroi", Doctorat thesis, Ecole Centrale de Lyon, France.

H. Iacovides and M. Raisee, Computation of flow and heat transfer in 2-D roughened passages. *2 nd Int. Symp on Turbulence Heat and Mass Transfer*, pages 21-30.1997.

Jones, W. and Launder, B.E., 1972, "The prediction of laminarization with a two equations model of turbulence", International Journal of Heat and Mass Transfer, vol. 15, pp. 301-314.

Kays,W.M., Crawford, M.E. 1993, "Convective Heat and Mass Transfer", McGraw Hill, INC., USA

Launder, B.E. and Spalding, D.B., 1974, "The numerical computation of turbulent flows", Computational Methods in Applied Mechanical Engineering, vol. 3, pp. 269-289

Liou, T.M. and Hwang, J.J, "Turbulent heat transfer augmentation and friction in periodic fully developed channel flows", Journal of Heat Transfer, Vol.114, pp.56-64, 1992.

Mellor, G.L., 1966, "The effects of pressure gradients on turbulent flow near a smooth wall", Journal of Fluid Mechanics, vol. 24, n^o 2, pp. 255-274

Nakayama, A., Koyama, H., 1984, "A wall law for turbulent boundary layers in adverse pressure gradients", AIAA Journal, vol. 22, n^o 10, pp. 1386-1389

Reynolds, O., 1895, "On The Dynamical Theory of Incompressible Viscous Fluids and the Determination of the Criterium" , Philosophical Transactions of the Royal Society of London, Series A, Vol 186, p. 123

S.V. Patankar, C.H. Liu, and E.M. Sparrow. Fully developed flow and heat transfer in ducts having streamwise-periodic variations of cross sectional area. J. Heat Transfer, 99:180-186, 1977.

7. Responsibility notice

The author(s) is (are) the only responsible for the printed material included in this paper